Theor Chem Acc (2001) 105:197–206
DOI 10.1007/s002140000194

Theoretical
Chemistry Accounts

Regular article

A quantum chemical study of the mechanism of manganese catalase

Per E. M. Siegbahn

Department of Physics, Stockholm University, Box 6730, 113 85 Stockholm, Sweden

Received: 12 July 2000 / Accepted: 12 July 2000 / Published online: 21 December 2000

Abstract. The catalytic mechanism of manganese catalase has been studied using the Becke's three parameter hybrid method with the Lee, Yang and Parr correlation functional. On the basis of available experimental information on the geometric and electronic structure of the active manganese dimer complex, different possibilities were investigated. The mechanism finally suggested consists of eight steps. In the first steps, the first hydrogen peroxide becomes bound and its O–O bond is activated. This occurs in a spin-forbidden process found to be common in many biological processes where the O–O bond is cleaved, and two general rules are formulated for the requirements for a low activation energy in this type of reaction. As the O–O bond is cleaved a hydroxyl radical is initially formed in the overall rate-limiting step of the catalytic cycle. This radical is then immediately and irreversibly quenched in a strongly exothermic step. In the subsequent steps, the second hydrogen peroxide becomes bound and its two O–H bonds are broken, leading to the formation of an O_2 molecule, which is released. Parallels between the reversal of the present O–O cleavage mechanism in manganese catalase and the recently suggested O–O bond formation in photosystem II are drawn.

Key words: Manganese catalase – Density functional theory – Mechanism – Hydroxyl radical – Modeling

1 Introduction

Catalases are metalloenzymes that protect the cell from oxidative damage by excess hydrogen peroxide produced during O_2 metabolism [1]. Hydrogen peroxide is destroyed resulting in the formation of oxygen and water in a disproportionation reaction:

$$2H_2O_2 \rightarrow 2H_2O + O_2 + \Delta E \ . \quad (1)$$

This reaction is quite exothermic (experimental enthalpy value 52 kcal/mol; theoretical value 51 kcal/mol) [2], which means that one or several steps in the catalytic cycle of the enzyme may have a large driving force. The dangerous chemistry that catalases are there to prevent is termed Fenton chemistry [3] and leads to a production of hydroxyl radicals that can be very toxic for the cells. There are two major classes of catalases. The most abundant one of these has an Fe protoporphyrin IX cofactor with a proximal tyrosinate ligand trans to the position where the substrate binds. In the first step of the most accepted mechanism, a reaction between the resting ferric state and hydrogen peroxide results in an O–O bond cleavage, forming an Fe(IV) = O structure and an additional radical either in the heme organic π system or on one of the neighboring amino acids [4]. This step has recently been studied in detail using quantum chemical methods [5] for the case of a proximal imidazole ligand as present in peroxidases such as in cytochrome c peroxidase and in ascorbate peroxidase. On the basis of the results of this investigation this step should have a rather low barrier and only a small driving force. In the next step of the mechanism suggested for heme catalases, O_2 should be formed from a second hydrogen peroxide following hydrogen abstraction by the oxo ligand. The overall disproportionation reaction as shown in Eq. (1) is thus suggested to be a result of two quite separate reactions. For heme catalases it should be the second of these reactions that has a large driving force. The mechanisms of heme catalases have been reviewed rather recently in the general context of metal sites in biology [6].

In the second major class of catalases there is instead an active dimanganese complex. This type of catalase has been isolated from the thermophilic eubacteria, for example, *Thermus thermophilus* [7, 8] and *Thermoleophilium album* [9], and from lactic acid bacteria, for example, *Lactobacillus plantarum* [10]. Crystal structures have been determined for the cases *T. thermophilus* [11] and *L. plantarum*. These structures show that both enzymes have a bridged binuclear manganese cluster (Fig. 1). During turnover the binuclear cluster cycles between two different sets of oxidation states, the reduced form, Mn_2(II,II), and the oxidized form, Mn_2(III,III), which

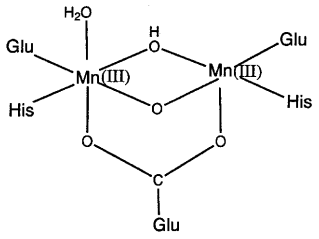

Fig. 1. The oxidized bridged binuclear manganese cluster of manganese catalase

are both, in principle, indefinitely stable. Electron paramagnetic resonance (EPR) studies reveal that the reduced form is weakly antiferromagnetically coupled. However, two excited-state EPR signals, from a triplet and a quintet, can also be observed [12]. The oxidized form is more strongly antiferromagnetically coupled and lacks an EPR signal [12, 13]. Manganese binuclear enzymes including manganese catalase have been reviewed rather recently [12], although before any actual crystal structure of catalase was available.

In the present study, the mechanism of manganese catalase is investigated by density functional theory. Several mechanisms have been suggested previously on the basis of experiments. In one of these mechanisms, internal protein residues play a key role as proton acceptors and donors [12]. In the first step, the substrate should bind directly to a terminal site on Mn(II) by displacement of a water ligand. The internal proton residue should then function as a proton acceptor from hydrogen peroxide. The cleavage of the O–O bond is suggested to occur after a critical step where the terminally ligated substrate swings in and forms a μ–η^2-peroxide. At this stage the O–O bond is broken in a process where the external residue back-delivers the proton to form product water. Protonation of μ-oxo and cleavage of the bridge is proposed to occur upon binding of the second substrate to a terminal Mn(III) site. Intramolecular two-electron transfer from hydroperoxide to reduce both Mn(III) ions, coupled to proton transfer to the external proton acceptor, should complete the cycle by generating O_2. In another proposed mechanism [13], the lability of the bridging group of the reduced complex is suggested to allow substitutional insertion of peroxide in this position. Isomerization of peroxide to the gem-protonation isomer is then suggested to sufficiently polarize the O–O bond for heterolytic bond cleavage. The second substrate then binds to the oxidized form as a terminal ligand and reduces the cluster in a two-electron step that results in the formation of a weakly coordinating terminal dioxygen as the product. A mechanism in which interconversion of Mn_2(II,II)(μ-OH)$_2$ and Mn_2(III,III)(μ-O)$_2$ core structures forms the basis of the catalytic cycle has also been suggested [14].

2 Computational details

The calculations were performed in three steps. First, an optimization of the geometry was performed using Becke's three parameter hybrid method with the Lee, Yang and Parr correlation functional (B3LYP) [15, 16]. Double-zeta basis sets were used in this step. In the second step the energy was evaluated for the optimized geometry using large basis sets, also at the B3LYP level. In the final step, polarization effects from the surrounding protein were evaluated using a dielectric cavity model. The calculations were carried out using the Gaussian 94 [17] and Gaussian 98 [18] programs.

In the B3LYP geometry optimizations, the LANL2DZ set of the Gaussian program, was used. For manganese this means that a nonrelativistic effective core potential (ECP) [19] was used. The valence basis set used for manganese in connection with this ECP is essentially of double-zeta quality. The rest of the atoms are described by standard double-zeta basis sets. In the B3LYP energy calculations the diffuse and polarization functions from the 6–311 + G(1d,1p) basis sets in the Gaussian program were added to the LANL2DZ basis sets. This basis set has a single set of polarization functions on all atoms including an f set on Fe, and also diffuse functions. This basis set is somewhat smaller than the one previously used for similar studies [20, 21], since it was found in the very large number of cases tried that the additional functions rarely, if ever, had any significant effect on the results. The small double-zeta basis set was used to determine the geometries since it is well known that final energies are very insensitive to the size of the basis set used for the geometry optimization [22, 23]. This was tested in a few cases for manganese catalase by using the large basis set used for the energies (except the Mn f set) also for the geometry, but the final relative energies hardly changed (see later).

Zero-point vibrational effects for the most important reaction steps were obtained by calculating molecular Hessians at the B3LYP level using the same basis set as for the geometry optimization. Since these calculations are quite time-consuming, in most cases they were performed on the smaller model where ammonia was used instead of imidazole as a model for the actual histidine ligands. As shown later, the modeling using ammonia gives nearly identical results to those obtained using imidazole for the catalase reactions. The glutamates were modeled by formates, which should be an excellent approximation. This was tested for most steps of the present catalase mechanism by using acetate models instead, and the results agreed with the formate results for both geometries and energies almost to within the convergence thresholds used (approximately 0.01 Å and 0.5 kcal/mol). The molecular Hessians were also used to optimize saddle-point structures and to define these as true transition states. Since very high self-consistent-field (SCF) convergence was not possible to achieve, small additional imaginary frequencies had to be tolerated (up to 20 cm^{-1}). The transition-state structures for the model with imidazole ligands were obtained by actually calculating Hessians for these larger systems. Entropy and other temperature effects were also obtained from the computed Hessians. Since they were not computed in all cases and, in general, were found to be small, they are not included in the energies in the figures and in the text, but are discussed separately later. Dielectric effects from the surrounding protein were obtained using the self-consistent-isodensity polarized continuum model (SCI-PCM) [24], using a dielectric constant of 4, and these effects are included in all the energies discussed later. It should finally be added that ferromagnetic coupling between the manganese spins was used throughout, since these wavefunctions are much easier to converge and the relative energetic effects of antiferromagnetic coupling for the present systems are quite negligible [25, 26]. For example, the effects of antiferromagnetic coupling on the geometries for both an Mn_2(IV,IV) and an Mn_2(V,IV) complex were within the convergence thresholds used and the effect on the O–H bond strength of a hydroxy ligand of one of these complexes was only 0.5 kcal/mol. For the present manganese complexes, which have lower oxidation states and, therefore, also weaker antiferromagnetic coupling, the effects should be even smaller. A very small effect of antiferromagnetic coupling was also noted recently for the Fe_2(IV,IV) complex in methane monooxygenase (MMO) [27].

3 Results and discussion

The mechanism of manganese catalase was investigated using two different chemical models. First, for explor-

atory purposes, the histidines were modeled by ammonia. In this simple model it is possible to do many more calculations in a reasonable time and also to calculate molecular Hessians and thereby locate and confirm proper transition states. In the larger model, used afterwards, the histidines were more accurately modeled using imidazoles. The results using both models are shown in the energetic scheme later. As it turned out, the results using the ammonia and the imidazole ligands are extremely similar, which supports this type of procedure. The glutamates were modeled by formates, and this was found to be an excellent approximation as tested by a comparison to the larger acetate model (see earlier).

During catalytic turnover, the dimer complex of manganese catalase is known to alternate between two different oxidation states. One of these is the reduced form with oxidation states Mn_2(II,II) and the other one is the oxidized form with oxidation states Mn_2(III,III). As a starting point for the investigation of the mechanism these two complexes were optimized. Since no X-ray structure is yet generally available, the starting point for these optimizations was taken from Fig. 1 in Ref. [13], where no distances are given. These distances would have been useful for deciding on the charge state of the complex, but apart from this a rather crude starting point is all that is needed for the geometry optimizations. Also, information about the second shell structure around the complex would have been useful when the role of possible external residues was investigated (see later).

The fully optimized structure for the reduced form is given in Fig. 2, where spin populations larger than 0.10 are also shown. When the hydrogen atoms were added to the X-ray structure, the metal complexes were assumed to be neutral in the low dielectric medium of the enzyme [20, 21], owing to the lack of any direct experimental information on this point. A positively charged complex was also tested for the rate-limiting step (see later). Since the carboxylates are almost always negative and the histidines neutral there are essentially only two possible choices for placing the hydrogen atoms. The best choice found is the one shown in the figure with one bridging hydroxide and one bridging water, and where the bridging water is trans to the histidines. The alternative choice, with a bridging hydroxyl group trans to the histidines was found to have a less favorable energy. The reason is that the hydroxyl group has a larger trans effect and, therefore, prefers to occupy the position trans to the empty position on the second manganese. The spin populations on manganese are 4.84 and 4.81, which are typical for Mn(II). Only one other spin is larger than 0.10 and this is the one for the bridging hydroxide. There are two strong hydrogen bonds, both between carboxylates and water. One is between the terminal carboxylate of Glu36 and a terminal water on one manganese and the other between the terminal carboxylate of Glu155 on the other manganese and the bridging water. These two hydrogen bonds are of importance for the mechanism discussed later and are expected to be stronger and, therefore, more important than possible hydrogen bonds to second-sphere ligands. The imidazoles are not involved in hydrogen bonding to other ligands, which is one important reason why these can be modeled very well by ammonia.

The oxidized structure of the manganese complex is shown in Fig. 3. For this form of the complex there are several possibilities to place the hydrogen atoms while keeping a neutral complex. In the best choice found, the bridging hydroxyl which has a weaker trans effect than the oxo group is placed trans to the imidazoles. It is interesting to note that the same type of trans effect has recently been noted for the case of iron dimer complexes in MMO and ribonucleotide reductase [29], which are structurally quite similar to the present dimer complex. This trans effect could be one reason the histidines are trans to the substrate pocket in MMO. Going back to catalase, the spins on manganese are 3.90 and 3.83, typical for Mn(III). In this case the only other spin larger than 0.10 is on the bridging carboxylate of Glu70, which has a spin of 0.13. Since Mn(III) is Jahn–Teller (JT) active, one weak JT axis can be identified on each manganese. On both manganese, this axis is perpendicular to the bridging plane, for one manganese pointing along the Mn–H_2O direction and for the other along the empty coordination site. The existence and directions of the weak JT axis play important roles for the

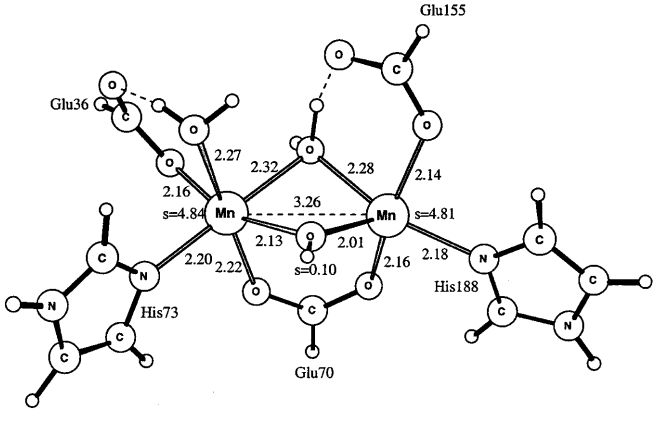

Fig. 2. Optimized structure for the reduced Mn_2(II,II) active site of manganese catalase

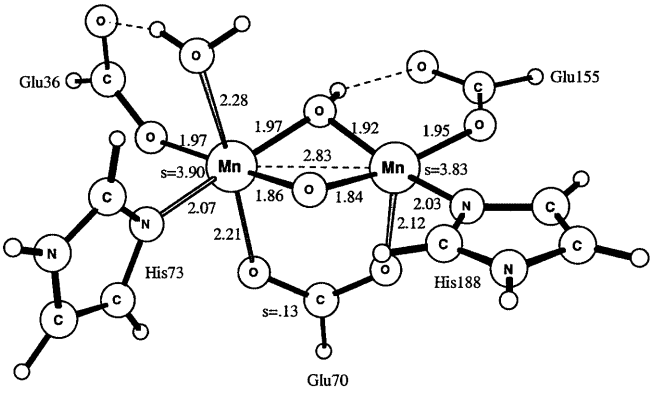

Fig. 3. Optimized structure for the oxidized Mn_2(III,III) active site of manganese catalase

mechanism, as usual for redox-active Mn-complexes [26, 28]. It is interesting to note that the distances along the weak JT axis are quite similar to the ones for Mn(II) in the reduced form, while the other distances have shortened substantially in the oxidized form.

The first step of the mechanism for manganese catalase that is suggested on the basis of the present calculations is shown in Fig. 4. In this step an incoming hydrogen peroxide simply replaces the bridging water of the reduced Mn_2(II,II) form. This has previously been suggested on the basis of experiments [13]. Since a water ligand in a manganese complex with oxidation states as low as II is quite loosely and flexibly coordinated, the substitution reaction was assumed to occur without any appreciable barrier. The five-coordination of one of the manganese in the present complex is one example of this flexibility. In fact, increasing the distance between the bridging water and one of the manganese atoms by more than 0.5 Å increases the energy by less than 1 kcal/mol. Only the reactant and product were therefore determined for this step. With the imidazole model, this reaction is calculated to be weakly exothermic by 0.3 kcal/mol. The product hydrogen peroxide is bridging and is hydrogen-bonded to Glu155 like the bridging water is for the reduced form in Fig. 2. It is also hydrogen-bonded with its other oxygen to the terminal water and with the hydrogen on this oxygen to the bridging hydroxide. Hydrogen peroxide is thus rather firmly bonded to the complex and is well prepared for activation.

It is in the second step of the mechanism, that the O–O bond of hydrogen peroxide should be broken. Assuming ferromagnetic coupling, which is an excellent approximation for these systems, the neutral Mn_2(II,II) reactant will have spin 11, while the ground state of the final Mn_2(III,III) product of the O–O bond cleavage reaction will have spin 9. These ground states follow from the weak ligand field in these complexes. A spin-crossing is therefore needed at some point in this process. For the present system this is required irrespective of whether the cleavage is homolytic, leading to two hydroxyl ligands, or if it is heterolytic, leading to one oxo ligand and one water molecule. The situation is quite different for heme-containing peroxidases where the ligand field is much stronger and the splitting between relevant spin states therefore quite different. A heterolytic cleavage of the type found for H_2 in NiFe hydrogenases [30], which does preserve the spin, can safely be ruled out for manganese catalase, since this would require the unlikely formation of a cationic hydroxyl ligand. For spin-crossing reactions of the present type two general rules can be formulated concerning the requirements for a low barrier [31, 32]. The first one of these says that either the excited state of the reactant corresponding to the product ground state (the low-spin state) or the excited state of the product corresponding to the reactant ground state (the high-spin state) has to be low lying. The second rule for a low barrier is less fundamental and is mainly based on previous experience, which means that exceptions may exist. It says that a low-lying transition state (with one imaginary frequency) must exist on at least one of the crossing spin-surfaces. The alternative, that none of the crossing spin-surfaces has an low-lying transition state, and that a low barrier is still found as determined by the spin-crossing point, should at least be very unusual. To clarify, it should be added that the second rule does not exclude the possibility that the barrier defining the rate of the reaction may actually be determined by the spin-crossing point, but says that in addition to this barrier there should also be a low-lying transition state on one of the spin-surfaces. There are two rationales for this empirical rule. First, it is reasonable that with two surfaces that rise steeply towards the spin-crossing point there will be a high barrier. If, on the other hand, one of the surfaces has a low-lying transition state, at least this surface will be flat, or may even go down, in the bond-cleavage region. The second rationale is connected to the first one, and concerns the spin-crossing probability. If the surfaces cross with a steep descent, the spin-crossing probability will be low and will therefore lead to a high effective barrier (low rate) [32–34]. The largest spin-crossing probability is, in fact, obtained if both surfaces are flat, but if at least one of the surfaces is flat this will increase the probability.

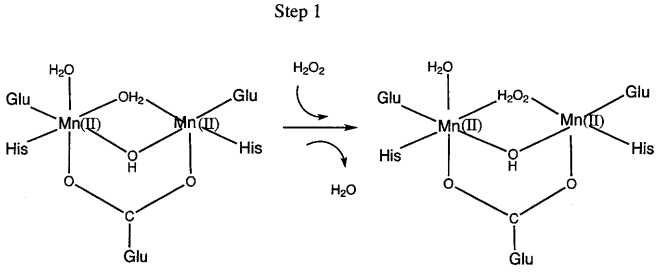

Fig. 4. Step 1 of the mechanism suggested for manganese catalase

In the reaction where the O–O bond of hydrogen peroxide is cleaved by the manganese catalase complex, the choice given in the first rule is very simple. Since the reaction is found to be strongly exothermic by more than 40 kcal/mol, there is a good chance that the excited state of the product will be quite low-lying compared to the reactant ground state, and this is found to be the case. The excited state of the product is actually found to be 3.9 kcal/mol lower than the reactant ground state. The reaction should thus occur on the reactant ground-state surface, leading to an excited state of the product. Since the lowest excited state of the product with the right spin has a hydroxyl radical ligand, the conclusion is that this radical will be the initial product of the O–O bond cleavage, which is one of the most important conclusions of the present study. The mechanism of step 2 is shown in Fig. 5 and the transition state in Fig. 6.

The transition state in Fig. 6 was quite difficult to locate and some further comments on this problem should be given here. A starting structure for the search of the transition state was obtained by increasing the O–O distance in steps of 0.10 Å until a maximum was found. At this point a molecular Hessian was calculated which had one imaginary frequency; however, using this Hessian and following the imaginary frequency led to a transition state which was actually one for electron transfer between the manganese centers rather than the

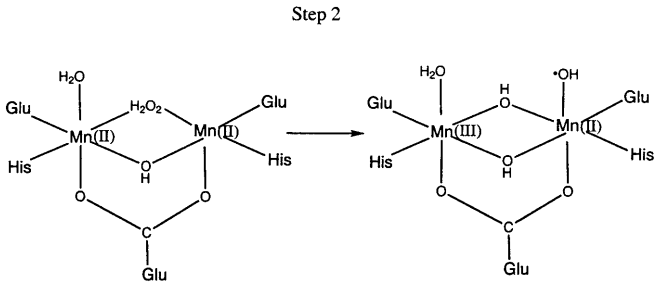

Fig. 5. Step 2 of the mechanism suggested for manganese catalase

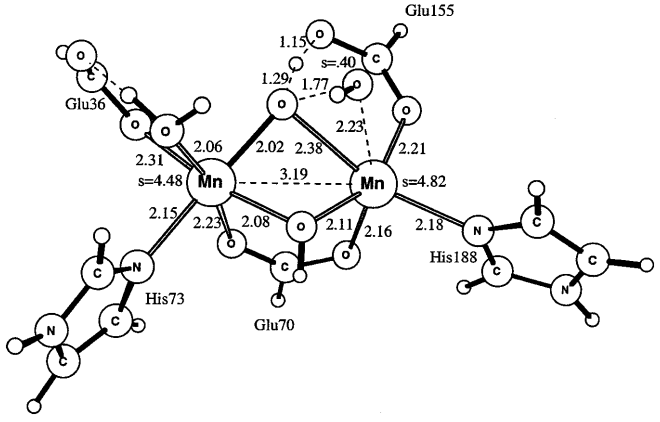

Fig. 6. Optimized transition state structure for the O–O activation of H_2O_2 in step 2

one defining the O–O bond cleavage. The O–O bond cleavage is instead initiated by electron transfer from Mn(II) to hydrogen peroxide, which requires a very specific geometry and is therefore difficult to locate. However, by also freezing the distance between the leftmost manganese and the closest oxygen of the peroxide in steps of 0.1 Å, the region for the electron transfer to the peroxide could be determined better. After the new determination of the Hessian at the saddle point of the two-dimensional surface, the transition state eventually converged to the structure in Fig. 6. The leading imaginary frequency of the Hessian is 544 cm^{-1} and one additional imaginary frequency of 20 cm^{-1} appeared as a result of low SCF convergence. A few characteristic features of this structure should be mentioned. The spin on the leftmost manganese of 4.48 is between the one typical for Mn(II) of 4.8 and of Mn(III) of 3.9 and shows that the system is in the process of sending the electron to the peroxide. The second manganese remains as Mn(II) during the entire O–O bond cleavage. The only other spin larger than 0.1 in the complex is located on the outermost oxygen of the peroxide (0.40) and shows that this is where the hydroxyl radical is being formed. An important structural feature of the transition state is that a proton is drawn towards the carboxylate of Glu155, which loses its contact to the second manganese somewhat. This is quite important and significantly lowers the barrier. The hydrogen bonding of Glu36 at the first manganese center also changes somewhat, leading to a decrease of the Mn–O distance for Glu36 from 2.11 Å for the Mn(II) reactant to 1.95 Å for the transition state in Fig. 6. This change, forced by the change of oxidation state, is simplified by a corresponding weakening of the hydrogen bond between Glu36 and the water ligand on this center. The O–H hydrogen-bond distance changes from 1.54 to 1.61 Å. The distances around the first manganese are overall between those of Mn(II) and Mn(III), in line with the change of spin. The potential surface after the transition state is extremely flat and the hydroxyl radical finally ends up with a distance of 2.24 Å to the second manganese.

The computed barrier height for the reaction going over the transition state in Fig. 6 is 15.4 kcal/mol. This is the highest barrier of all the steps in the catalytic cycle and limits the rate to about 30 s^{-1}. Experimentally, the rate of the catalytic cycle is 10^{4-5}, depending on the particular enzyme [35–37], which means that the rate is almost limited by diffusion [12]. The experimental barriers correspond to barriers in the range 10–12 kcal/mol, which means that the calculated barrier is 3–5 kcal/mol too high. The overestimation by B3LYP of the barrier for this type of reaction is in line with recent experience obtained for similar reactions for other systems where electron transfer is involved [38]. In order to see if a spin-crossing might occur before the actual transition state and lower the barrier somewhat, a calculation was performed for the low-spin state in the saddle-point geometry of the high-spin state, but the energy was much higher than for the high-spin state. This does not entirely rule out a spin-crossing before the transition state, but makes it very unlikely. As an alternative, the O–O bond cleavage of H_2O_2 was also tried at the empty coordination site of the rightmost manganese. This led to a barrier which is very close to the one for the transition state in Fig. 6, and is thus a valid alternative; however, the character of this transition state is almost identical to the one described earlier and, therefore, does not represent a significantly different mechanism, and for this reason this pathway is not discussed here further.

A third alternative mechanism was also tried, where the effect of an additional proton from an external proton donor [12] was investigated, by placing a proton on the outermost oxygen of H_2O_2 in the structure in Fig. 6. It turns out that the proton added moves over from H_2O_2 to Glu36, followed by O–O bond cleavage with a mechanism and barrier height which are very similar to those for the unprotonated system. It is concluded that an outside proton donor does not appear to help to lower the barrier. In the beginning of this section it was noted that the charge state of the complex remains an uncertain parameter. In the absence of any other evidence the complex was therefore chosen to be neutral. Since the neutral and positively charged complexes behave very similarly in the O–O bond-breaking step, it is concluded that the charge state of the complex does not appear to be an important factor in the present case. To deprotonate the complex before the O–O bond cleavage, and thus make the complex negative, should not be an advantage and has not been suggested by any previous investigator. It should finally be noted that the charge state for other systems can be important as, for example,

found recently for isopenicillin n synthase [39] and cytochrome c oxidase [40].

A number of attempts to find the transition state for O–O bond activation preceded the finding of the one in Fig. 6. These attempts were made on the basis of previous experience of O–O bond activations. In a recent study of heme peroxidases [5], the O–O bond was found to be cleaved by first deprotonating one of the oxygens and then protonating the other one, forming an oxo ligand and a water molecule in a heterolytic mechanism. In cytochrome c oxidase [40], a similar mechanism was found for the activation of O_2. In the initial attempts to break the O–O bond of hydrogen peroxide in manganese catalase, one of the oxygens was therefore first protonated by moving a proton from another ligand; however, both taking the proton from the terminal water and from the bridging hydroxyl was found to require too much energy. This result was independent of whether the other oxygen of the peroxide, the one hydrogen-bonded to Glu155, was deprotonated by this carboxylate or not. The heterolytic mechanism was therefore considered much less likely than the homolytic one.

Since the best mechanism to activate the O–O bond of hydrogen peroxide found here has a barrier that is 3–5 kcal/mol too high compared to experiments a few comments on the accuracy of the present methods, basis sets and models should be given. First, an error of 3–5 kcal/mol due to the use of the B3LYP method for a barrier of a complicated reaction like this is certainly possible on the basis of previous experience, even though it is slightly large. Second, since the basis set used for the geometries is rather small, a larger basis set was also tried. For the larger basis set two coordinates, O–O and Mn1–O, were held frozen from the smaller basis set in the geometry optimization of the transition state. Using the large basis set, described in Sect. 2, without the manganese f set but with polarization on all other atoms and also including diffuse functions, the barrier increased very slightly by 0.7 kcal/mol. This result is perfectly in line with previous experience gathered during a decade of quantum chemical modeling, including modeling of transition-metal complexes [22, 23], that the final energy is very insensitive to the quality of the geometry optimization. Concerning the model, there is first the question concerning the modeling of the ligands. Changing the models of the glutamates from formates to the larger acetates decreases the barrier by an insignificant 0.4 kcal/mol (compared to the total barrier of 15.4 kcal/mol), which can be considered to be within the normal convergence thresholds used in the calculations. The geometric changes are also insignificant. Changing the models of the histidines from imidazoles to the smaller ammonias, actually gave an identical (within 0.1 kcal/mol) barrier. The conclusion from these investigations is that the result is very stable with respect to basis set and chemical model. Since the result is so stable even with respect to modifications of the first layer ligands, it is assumed here that the effects of second-sphere ligands and also the rest of the enzyme should be rather small and that they should not qualitatively change the present mechanism. In a recent direct investigation [27] of the effect of a second-sphere hydrogen bond in MMO, previously suggested to be important [41], it was shown that this hydrogen bond was quite insignificant for the relative energies and structures. Unfortunately, careful comparisons of the effects of the surrounding enzyme in reactions similar to the present one hardly exist. However, there is a recent investigation of galactose oxidase, where the effect of the enzyme (modeled in its entirety) was shown to have quite insignificant effects on the mechanism [42]. Similar results were obtained for the same enzyme in another study [43]. Also, the quite small effects from the dielectric modeling repeatedly obtained in enzyme studies of reaction mechanisms (including the present one) clearly argues against large effects from the surrounding enzyme [20, 21]. The main possible errors of the present study should, therefore, firstly, be the possibility that B3LYP should unexpectedly fail for the present reaction or, secondly, be that a mechanism has not yet been thought of within the present model. However, not many fundamentally different mechanisms for activating the O–O bond are known and these have been considered here (see earlier).

As already indicated, step 3 of the catalase mechanism suggested here, is the spin-crossing leading to an Mn_2(III,III) product. This crossing, which should be very efficient, leads to a manganese-bound hydroxyl ligand, which will directly reorganize and combine with a proton on a bridging hydroxyl to form water and a bridging oxo ligand as indicated in Fig. 7. The water is pushed out from manganese since it is situated along the weak JT axis. This step is found to be exothermic by as much as 39.1 kcal/mol. Of the total exothermicity available for the catalase reaction (Eq. 1) of 52 kcal/mol, most of it is thus spent in this step. This is in contrast to the heme catalases, where the O–O bond-breaking step should have only a weak driving force [5]. The large exothermicity involved in the spin-crossing for manganese catalase means that this step is efficient and irreversible. The consequence is that the potentially dangerous hydroxyl radical is immediately quenched, which is obviously critical for the function of the enzyme.

With this mechanism of the O–O bond cleavage for manganese catalase, it becomes interesting to look at the reverse of this step and see if it has any implications for O–O bond formation in photosystem II (PSII), where a manganese complex with weak ligand field is also used. The most striking point in the reversal of steps 2 and 3,

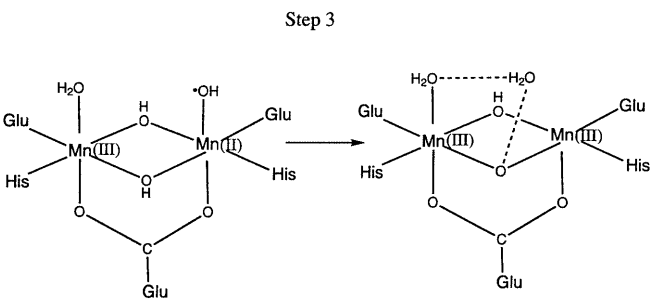

Fig. 7. Step 3 of the mechanism suggested for manganese catalase

is that the O–O bond formation should be preceded by the formation of a hydroxyl radical. Clearly, a direct reversal of step 3 for manganese catalase is not applicable in a single step for PSII since the barrier would be over 50 kcal/mol; however, a mechanism for O–O bond formation in PSII which still has many similarities to the reversal of steps 2 and 3 has been suggested. In this mechanism, the energy made available to the manganese complex through the photon absorptions at the reaction center and the subsequent charge separations in the lower states is used to pump up the energy of the complex so that for the S_3 state a bridging oxyl radical is created [26, 28]. It is suggested that in the O–O bond-formation step the radical is first transferred to a hydroxyl radical in a low-energy step, after which it combines with a hydroxide ligand to form the O–O bond in a transition state similar to the one in Fig. 6. Even though the existence of an oxygen-based radical in S_3 is still controversial, there are also experimental indications of such a radical [44–46].

Step 4 of the mechanism suggested is shown in Fig. 8. As indicated, this is a rather trivial step, where the loosely bound water is replaced by another hydrogen peroxide, the second one in the overall reaction (Eq. 1). Owing to favorable hydrogen bonding for the peroxide, this step is found to be exothermic by 4.4 kcal/mol. The hydrogen-bond distance for the hydrogen peroxide to the bridging oxo group is, for example, quite short at 1.39 Å. At this stage, this strongly hydrogen bonding O–H bond of hydrogen peroxide is heterolytically cleaved. In this way, the oxidation states and, therefore, also the spin can be conserved, in contrast to the reaction in steps 2 and 3. The optimized transition-state structure for the O–H bond cleavage is shown in Fig. 9 and the overall step 5 reaction in Fig. 10. The barrier for this step is 8.9 kcal/mol, corresponding to a rate calculated from transition state theory of 10^6 s^{-1}. There is a single imaginary frequency of 198 cm^{-1} for the Hessian used to determine the transition state.

An interesting aspect of the reaction in step 5 is that the active Mn(III) is forced to change the direction of the weak JT axis. In the reactant, this axis points towards the empty coordination site; however, the product needs to bind the peroxide fragment at this site and it therefore turns this into a strongly binding site. Instead, the choice of the direction of the weak JT axis for the product is given by the bond to the Glu155 oxygen and the bond to the bridging hydroxyl formed in the O–H bond-breaking

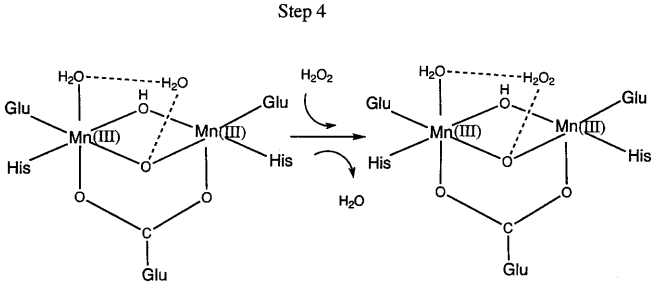

Fig. 8. Step 4 of the mechanism suggested for manganese catalase

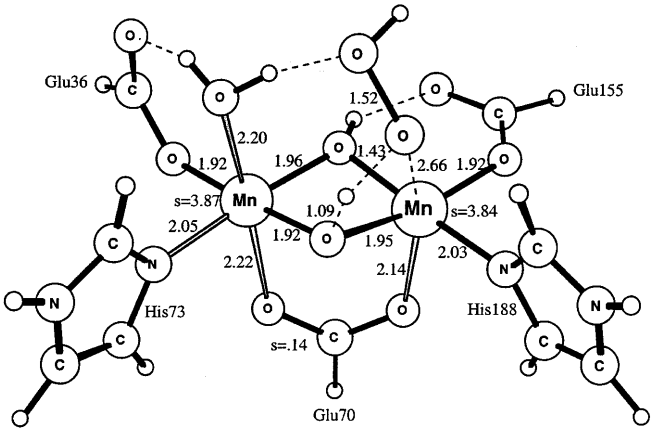

Fig. 9. Optimized transition-state structure for the O–H activation of H_2O_2 in step 5

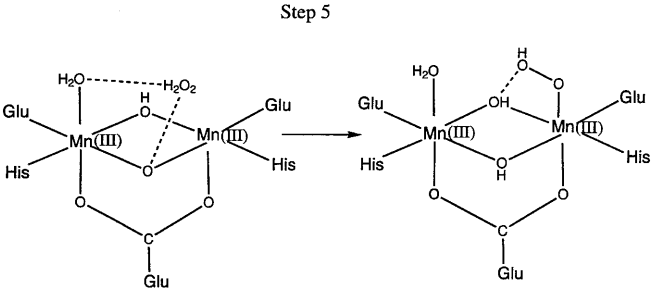

Fig. 10. Step 5 of the mechanism suggested for manganese catalase

process. To simplify this change of direction of the JT axis, the hydrogen bonding between Glu155 and the other bridging hydroxyl is quite important. Before the heterolytic cleavage of the O–H bond this hydrogen-bond distance is 1.82 Å and it changes to 1.49 Å after the reaction. The Mn–O distance for Glu155 is 1.94 Å before and 2.14 Å after the reaction. The negative carboxylate of Glu155 can thus compensate for the loss of electrostatic bonding to the manganese center by a corresponding increase in electrostatic hydrogen bonding. Simultaneously to these changes, the distance between the active manganese and the oxygen of Glu70 changes from 2.10 to 2.00 Å.

The only part remaining to complete the cycle of the catalase mechanism is to form an oxygen molecule from the OOH peroxide ligand bound to manganese at the end of step 5. The first part of this process is described in Fig. 11 as step 6. This step can be described as an electron transfer from one oxygen of the peroxide to manganese, coupled with a proton transfer from the other oxygen of the peroxide to a bridging hydroxide, leading to a bridging water. To perform this step, the transition state shown in Fig. 12 needs to be passed. Also this transition state was quite complicated to locate and required several Hessian evaluations. It is obvious that the O–H and O–O distances are important distances that vary along the reaction pathway, but the Mn–O distance is also a key geometrical parameter. The Mn–O distance is important mainly to control the electron transfer to manganese. For

the reactant in step 6, this Mn–O distance is 1.89 Å, at the transition state 2.11 Å and for the product 2.21 Å. In line with this change, the spin on manganese varies from 3.95 to 4.54 and to 4.79. The corresponding change on the peroxide is from −0.09 to −0.70 and to −0.95. Along the reaction pathway, the distances around the active manganese also increase from those typical for Mn(III) to those for Mn(II). This reaction thus couples an unusually large number of distance variations, which was one reason why it was difficult to locate. The calculated barrier for this step is 6.1 kcal/mol and the reaction is found to be endothermic by 3.6 kcal/mol. The Hessian of the transition state structure in Fig. 12 has only one imaginary frequency (460 cm^{-1}).

As seen in Fig. 11, the product of step 6 is an Mn_2(III,II) complex with the O_2^- radical ligand bound to the Mn(II) center. Because of this bond it might have appeared more natural for the product to have been Mn_2(II,III), with the oxidation states switched. In fact this change of oxidation states leads to a complex which is 4.4 kcal/mol more stable. For this reason, several attempts were made to find a transition state that directly linked the reactant of step 6 with the lowest energy product Mn_2(II,III) but these were all unsuccessful. The reason for this is that the electronic coupling between the peroxide and the second manganese, required to make this electron transfer, is too weak.

Instead the switch of oxidation states is described here as the subsequent step 7 and is shown in Fig. 13.

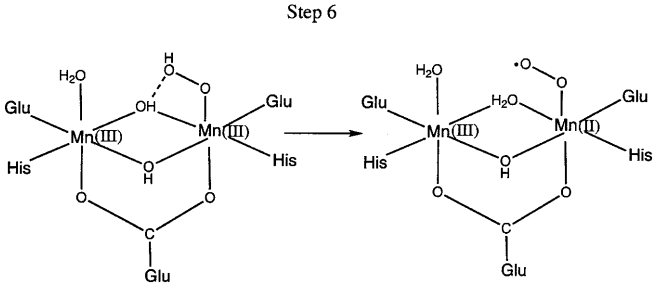

Fig. 11. Step 6 of the mechanism suggested for manganese catalase

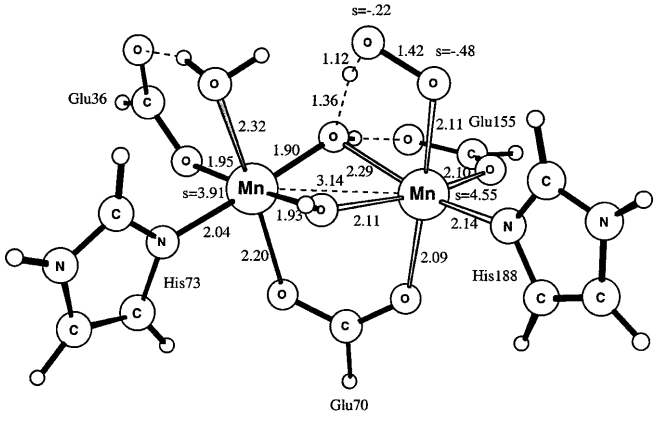

Fig. 12. Optimized transition-state structure for the formation of O_2 in step 6

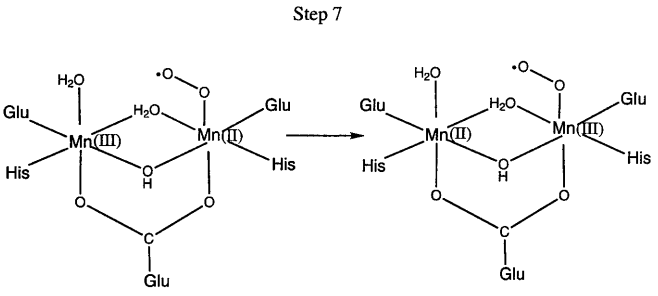

Fig. 13. Step 7 of the mechanism suggested for manganese catalase

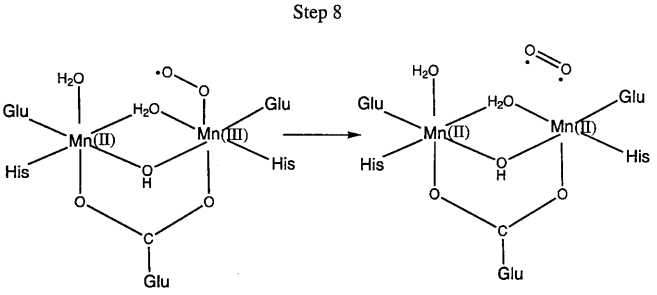

Fig. 14. Step 8 of the mechanism suggested for manganese catalase

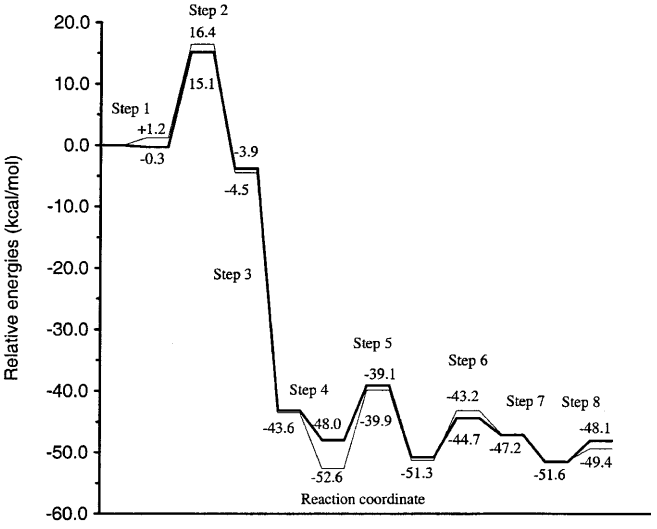

Fig. 15. Energy diagram for the mechanism suggested for manganese catalase. The results using the imidazole model are marked with the *thick line* and those for the ammonia model with the *thin line*

No attempt was made to locate the transition state involved in step 7, but the barrier is expected to be very low. In a recent study, electron transfer between manganese centers was studied for an Mn_2(II,III) as shown in Fig. 1 but with two bridging hydroxides. In that case the barrier for electron transfer was found to be only 1.9 kcal/mol. The reaction pathway was found to involve a strongly concerted motion of eight manganese–ligand distances in the complex. It can finally be added that the spin on the peroxide increases in step 7 from about 1.0 in the reactant to 1.4 in the product, showing

that the spin has changed almost half the way towards that of O_2, which has a spin population of 2.0.

The only step remaining is the one shown in Fig. 14, in which the O_2 molecule is released and the manganese complex returns to the original Mn_2(II,II) form it had at the start of step 1. In the calculations, this step is endothermic by 3.5 kcal/mol without temperature effects and occurs without any additional barrier; however, this is the only step where temperature has significant effects, and when these are added the step becomes exothermic by 1.3 kcal/mol. In particular, the entropy effects are as large as 6.0 kcal/mol. This is not unexpected since O_2 becomes almost free in this process. Since the effects are so large, there could also be a small entropy-dependent barrier involved for the dissociation, which is not possible to determine accurately in the present type of calculations.

4 Conclusions

The calculated energies of the proposed catalytic cycle of manganese catalase are shown in Fig. 15. The results are displayed for the small model with ammonia ligands and for the larger model with imidazole ligands. As seen in the figure, the results using the two models are strikingly similar. Clearly, the electronic structure effects of imidazole ligands are almost perfectly modeled by ammonia. However, even if the direct electronic structure effects had been identical, the results could still have differed if ammonia had become involved in artificial hydrogen bondings, however, this does not happen for the present model of manganese catalase. Artificial hydrogen bonds to ammonia may be very difficult to avoid for other systems, and in previous studies the results for ammonia ligands have therefore differed much more from for using imidazole ligands [20, 47].

The most interesting part of the mechanism suggested here for the catalytic cycle of manganese catalase occurs in steps 2 and 3, where the O–O bond of the first hydrogen peroxide in the overall reaction (Eq. 1) is cleaved. Owing to the spin-forbidden nature of this reaction, going from Mn_2(III,III), the process occurs in two steps. It is suggested that in the first step a hydroxyl radical is formed in a slightly exothermic reaction with a calculated barrier of 15 kcal/mol, which is the rate-limiting step of the entire cycle. Since the production of a hydroxyl radical is potentially dangerous, the radical must be quenched immediately after it is produced. To do this very effectively and irreversibly, a large part of the available exothermicity of the catalytic cycle is used up in this quenching step.

The remaining steps of the catalytic cycle, after the O–O bond cleavage has been completed, are quite fast. In steps 4 and 5, the second hydrogen peroxide in the reaction expressed by Eq. (1) is bound to the complex and one of its O–H bonds is cleaved by a heterolytic mechanism which preserves the spin. The barrier for this step is 8.9 kcal/mol. In step 6, the second O–H bond is cleaved with a barrier of 6.1 kcal/mol, leading to the formation of a bound peroxide with a spin population of about 1. In step 7 the oxidation states of the manganese centers are switched, leading to an increase of the spin on the peroxide. Finally, O_2 is formed in step 8 in a process which only becomes exothermic after the relatively large entropy effects of 6 kcal/mol have been added.

One of the most interesting aspects of the mechanism of manganese catalase is to see to what extent one can learn something from this process for the reverse one of O–O bond formation in PSII. It turns out that there are surprisingly many similarities between the catalase process found here and the mechanism recently suggested for PSII [26], even though the oxidation states are quite different. In the present mechanism of manganese catalase, a hydroxyl radical is produced in the O–O bond-cleavage step, while in the mechanism suggested for PSII an oxygen-based radical is a precursor for the O–O bond formation. To reach this radical precursor in S_3, which can be compared to climbing up from the reactant of step 4 backwards to the product of step 3 in Fig. 15, the manganese cluster in PSII can use the energy made available to it by the photon absorptions in the S states preceding S_3.

References

1. Voet D, Voet JG (1995) Biochemistry. Wiley, New York
2. Curtiss LA, Raghavachari K, Trucks GW, Pople JA (1991) J Chem Phys 94: 7221–7230
3. Walling C (1975) Acc Chem Res 8: 125
4. Sono M, Roach MP, Coulter ED, Dawson JH (1996) Chem Rev 96: 2841–2887
5. Wirstam M, Blomberg MRA, Siegbahn PEM (1999) J Am Chem Soc 121: 10178–10185
6. Holm RH, Kennepohl P, Solomon EI (1996) Chem Rev 96: 2239–2314
7. Barynin VV, Grebenko AI (1986) Dokl Akad Nauk SSSR 286: 461–464
8. Barynin VV, Vagin AA, Melik-Adamyan WR, Grebenko AI, Khangulov SV, Popov AN, Adnrianova ME, Vainshtein BK (1986) Sov Phys Dokl 81: 457–459
9. Allgood GS, Perry JJ (1986) J Bacteriol 168: 563–567
10. Kono Y, Fridovich I (1983) J Biol Chem 258: 6015–6019
11. Barynin VV, Hempstead PD, Vagin AA, Antonyuk SV, Melik-Adamyan WR, Lamzin VS, Harrison PM, Artymiuk PJ (1997) J Inorg Biochem 67: 196
12. Dismukes GC (1996) Chem Rev 96: 2909–2926
13. Whittaker MM, Barynin VV, Antonyuk SV, Whittaker JW (1999) Biochemistry 38: 9126–9136
14. Meier AE, Whittaker MM, Whittaker JW (1996) Biochemistry 35: 348–360
15. (a) Becke AD (1988) Phys Rev 38: 3098; (b) Becke AD (1993) J Chem Phys 98: 1372; (c) Becke AD (1993) J Chem Phys 98: 5648
16. Stevens PJ, Devlin FJ, Chablowski CF, Frisch MJ (1994) J Phys Chem 98: 11623
17. Frisch MJ, Trucks GW, Schlegel HB, Gill PMW, Johnson BG, Robb MA, Cheeseman JR, Keith T, Petersson GA, Montgomery JA, Raghavachari K, Al-Laham MA, Zakrzewski VG, Ortiz JV, Foresman JB, Cioslowski J, Stefanov BB, Nanayakkara A, Challacombe M, Peng CY, Ayala PY, Chen W, Wong MW, Andres JL, Replogle ES, Gomperts R, Martin RL, Fox DJ, Binkley JS, Defrees DJ, Baker J, Stewart JP, Head-Gordon M, Gonzalez C, Pople JA (1995) Gaussian 94, revision B.2. Gaussian, Pittsburgh, Pa
18. Frisch MJ, Trucks GW, Schlegel HB, Scuseria GE, Robb MA Cheeseman JR, Zakrzewski VG, Montgomery JA Jr, Stratmann RE, Burant JC, Dapprich S, Millan JM, Daniels AD, Kudin KN, Strain MC, Farkas O, Tomasi J, Barone V, Cossi

M, Cammi R, Mennucci B, Pomelli C, Adamo C, Clifford S, Ochterski J, Petersson GA, Ayala PY, Cui Q, Morokuma K, Malick DK, Rabuck AD, Raghavachari K, Foresman JB, Cioslowski J, Ortiz JV, Stefanov BB, Liu G, Liashenko A, Piskorz P, Komaromi I, Gomperts R, Martin RL, Fox DJ, Keith T, Al-Laham MA, Peng CY, Nanayakkara A, Gonzalez C, Challacombe M, Gill PMW, Johnson B, Chen W, Wong MW, Andres JL, Head-Gordon M, Replogle ES, Pople JA (1998) Gaussian 98. Gaussian, Pittsburgh, Pa
19. Hay PJ, Wadt WR (1985) J Chem Phys 82: 299
20. Siegbahn PEM, Blomberg MRA (1999) Annu Rev Phys Chem 50: 221–249
21. Siegbahn PEM, Blomberg MRA (2000) Chem Rev 100: 421–437
22. Siegbahn PEM (1996) In: Prigogine L, Rice SA (eds) Advances in chemical physics, vol XCIII. Wiley, New York, pp 333–387
23. Bauschlicher CW Jr, Ricca A, Partridge H, Langhoff SR (1997) In: Chong DP (ed) Recent advances in density functional methods, part II. World Scientific, Singapore, p 165
24. (a) Wiberg KB, Rablen PR, Rush DJ, Keith TA (1995) J Am Chem Soc 117: 4261; (b) Wiberg KB, Keith TA, Frisch MJ, Murcko M (1995) J Phys Chem 99: 9072
25. Blomberg MRA, Siegbahn PEM, Styring S, Babcock GT, Akermark B, Korall P (1997) J Am Chem Soc 119: 8285–8292
26. Siegbahn PEM (2000) J Inorg Chem 39: 2923–2935
27. Siegbahn PEM (2000) J Inorg Biochem (in press)
28. Siegbahn PEM, Crabtree RH (1999) J Am Chem Soc 121: 117–127
29. Siegbahn PEM (1999) J Inorg Chem 38: 2880–2889
30. Pavlov M, Siegbahn PEM, Blomberg MRA, Crabtree RH (1998) J Am Chem Soc 120: 548–555
31. Siegbahn PEM, Blomberg MRA (2000) In: Eriksson LA (ed) Theoretical chemistry – processes and properties of biological systems. Elsevier, Amsterdam (submitted)
32. Siegbahn PEM, Crabtree RH (2000) In: Meunier B (ed) Metal–oxo and metal–peroxo species in catalytic oxidations. Springer, Berlin Heidelberg New York (in press)
33. Mitchell SA (1992) In: Fontijn A (ed) Gas-phase metal reactions, Elsevier, Amsterdam, pp 227–252
34. Mitchell SA, Blitz MA, Siegbahn PEM, Svensson MJ (1994) Chem Phys 100: 423–433
35. Shank M, Barynin V, Dismukes GC (1994) Biochemistry 38: 15433–15436
36. Penner-Hahn JE (1992) In: Pecoraro VL (ed) Manganese redox enzymes, Verlag Chimie, New York
37. Allgood GS, Perry JJ (1998) J Bacteriol 168
38. Blomberg MRA, Siegbahn PEM, Babcock GT, Wikström M (2000) J Am Chem Soc (submitted)
39. Wirstam M, Siegbahn PEM (2000) J Am Chem Soc 122: 8539–8547
40. Blomberg MRA, Siegbahn PEM, Babcock GT, Wikström M (2000) J Inorg Biochem (in press)
41. Dunietz BD, Beachy MD, Cao Y, Whittington DA, Lippard SJ, Friesner RA (2000) J Am Chem Soc 122: 2828–2839
42. Rothlisberger U, Carloni P, Doclo K, Parinello M (2000) J Biol Inorg Chem 5: 236–250
43. Himo F, Eriksson LA, Maseras F, Siegbahn PEM (2000) J Am Chem Soc 122: 8031–8036
44. Yachandra VK, Sauer K, Klein MP (1998) Chem Rev 96: 2927–2950
45. (a) Styring SA, Rutherford AW (1988) Biochemistry 27: 4915–4923; (b) Evelo RG, Styring SA, Rutherford AW, Hoff AJ (1989) Biochim Biophys Acta 973: 428
46. Sharp RR (1992) In: Pecoraro VL (ed) Manganese redox enzymes. VCH, New York, pp 177–196
47. Lind T, Siegbahn PEM, Crabtree RH (1999) J Phys Chem103: 1193–1202